

fluence of nearby particle thresholds must be properly taken into account. However, the matrix elements we calculate are in reasonable agreement with published experimental values.<sup>12</sup>

We conclude by noting that although the pure isovector one-particle INC matrix elements are substantially larger than the two-particle INC matrix elements, isospin mixing of antianalog states [see formulas (1)–(4)] invariably involves differences of these matrix elements which are of similar size for both types. This explains why isospin-forbidden particle decay widths indicate comparable isotensor and isovector matrix elements in light nuclei where antianalog mixing is important.

The success of this simple model based on the Coulomb force alone makes it unlikely that isospin mixing in these light nuclei can provide unambiguous evidence for charge dependence in the short-range nuclear force.

We would like to acknowledge very helpful discussions with G. T. Garvey, M. Harvey, G. Miller, and J. P. Schiffer. One of us (A.B.M.) thanks the staff of the University of Washington for their hospitality during a very pleasant sum-

mer visit. The University of Washington laboratory is supported in part by the U. S. Energy and Research Development Administration.

<sup>1</sup>G. Bertsch and A. Z. Mekjian, *Annu. Rev. Nucl. Sci.* **22**, 25 (1972); N. Auerbach and A. Lev, *Phys. Lett.* **34B**, 13 (1971).

<sup>2</sup>E. G. Adelberger, in *Proceedings of the International Conference on Nuclear Structure and Spectroscopy, Amsterdam, 1974*, edited by H. P. Blok and A. E. L. Dieperink (Scholar's Press, Amsterdam, 1974), p. 641.

<sup>3</sup>A. B. McDonald *et al.*, *Nucl. Phys.* **A273**, 477 (1976).

<sup>4</sup>P. G. Ikossi *et al.*, *Nucl. Phys.* **A274**, 1 (1976).

<sup>5</sup>R. L. McGrath *et al.*, *Phys. Rev. C* **1**, 184 (1971).

<sup>6</sup>S. J. Freedman *et al.* to be published.

<sup>7</sup>G. T. Garvey and I. Kelson, *Phys. Rev. Lett.* **16**, 197 (1966).

<sup>8</sup>R. Sherr, *Phys. Rev. C* **16**, 1159 (1977).

<sup>9</sup>H. Weigmann, R. L. Macklin, and J. A. Harvey, *Phys. Rev. C* **14**, 1328 (1976).

<sup>10</sup>P. A. Dickey, E. G. Adelberger, and J. E. Bussoletti, to be published.

<sup>11</sup>F. Barker, *Aust. J. Phys.* **31**, 27 (1978).

<sup>12</sup>F. C. Barker, *Nucl. Phys.* **83**, 418 (1966); E. G. Adelberger *et al.*, *Phys. Rev. C* **15**, 484 (1977); G. J. Wagner *et al.*, *Phys. Rev. C* **16**, 1271 (1977).

## Nuclear Excitation Rate

G. D. Doolen

*Los Alamos Scientific Laboratory, Los Alamos, New Mexico 87545*

(Received 27 February 1978)

The rate at which the first nuclear excited state becomes populated is calculated as a function of temperature and compression for <sup>238</sup>U.

When a nucleus in its ground state is placed in a high-temperature environment, the excited states of the nucleus approach an equilibrium population whose ratio to the ground-state population is given by

$$\frac{(2J_i + 1) \exp(-E_i/kT)}{(2J_0 + 1)}, \quad (1)$$

where  $J_i$  and  $J_0$  are the spins of the  $i$ th excited state and the ground state, respectively.  $E_i$  is the energy of the excited state above the ground state.  $T$  is the temperature and  $k$  is the Boltzmann constant.

The objective here is to examine the processes by which equilibrium is obtained and to calculate the nuclear excitation rate of a nucleus. I define the nuclear excitation rate as the initial rate at

which ground-state nuclei become excited to the first excited state when the pure isotopic material is compressed to  $c$  times its normal density and heated to a temperature  $T$ . As an example, I consider the isotope <sup>238</sup>U with  $0.3 \leq c \leq 100$  and  $0.05 \text{ keV} \leq T \leq 30 \text{ keV}$ .

Two physical processes dominate the nuclear excitation rate. One process is radiation excitation in which a photon from the blackbody spectrum is absorbed by the nucleus. The radiation excitation depends on the radiation temperature and the nuclear wave functions for the two states involved in the transition. The other process is inverse internal conversion, in which an electron in the continuum or an excited state makes the transition to a lower-energy state and gives its transition energy to the nucleus. The inverse

internal conversion process in addition depends on the electronic wave functions, which are sensitive to compression as well as temperature.

*The nuclear decay rate and its modification for temperature dependence.*—The total nuclear transition rate (excluding pair production, etc.) for decay of a nuclear excited state is<sup>1</sup>

$$T_{J_i \rightarrow J_f} = 8\pi \sum_{L \geq 1} \left\{ \left( \frac{\omega^{2L+1}(L+1)}{L[(2L+1)!!]^2} |\gamma(\pi, L, J_i - J_f)|^2 \right) \left( 1 + \sum_{n_0 k_0} \alpha_{n_0 k_0}(\pi L) \right) \right\}. \quad (2)$$

Here  $\omega$  is the nuclear transition energy,  $|\gamma(\pi, L, J_i - J_f)|^2$  is the reduced transition probability (which contains the nuclear information),  $\pi$  and  $L$  are the parity and angular momentum of the transition, and  $J_i$  and  $J_f$  are the initial and final nuclear spins. The term,  $\alpha_{n_0 k_0}(\pi L)$ , is the internal conversion coefficient (which contains atomic electron information). The atomic orbital is specified by the quantum numbers,  $n_0 k_0$ . The term 1, in  $[1 + \sum_{n_0 k_0} \alpha]$ , is associated with a purely radiative transition.

Equation (1) requires modification when the atom is in equilibrium with a blackbody radiation field and electron field at temperature  $T$ . First, note that the nuclear matrix element  $\gamma(\pi, L, J_i - J_f)$  does not change. It depends on the expectation value of a nuclear operator between nuclear wave functions which are not significantly affected by the temperatures or compressions considered here. Second, the radiative term, 1, is replaced by the term  $n+1$ , where  $n$  is the number of photons in the sample with energy equal to the difference in energy between the initial state,  $J_i$ , and the final state,  $J_f$ . Since  $n$  is positive this factor always enhances the transition probability and decreases the half-life.

Third, the term containing the internal conversion coefficients becomes modified. The original sum,  $\sum_{n_0 k_0} \alpha_{n_0 k_0}$ , describes the bound-free electron transition in which a bound electron is ejected into the continuum. At high temperatures, the bound states have a probability less than one of being occupied. I call this probability  $P_{n_0 k}$ . The energy state into which the bound electron is ejected also has a finite probability of being occupied. I call this probability  $P_k$ . Because of the Pauli exclusion principle, which forbids two electrons with the same quantum numbers, we must multiply  $\alpha_{n_0 k_0}$  by the probability of the final state being empty,  $1 - P_k$ . Hence the original sum,  $\sum_{n_0 k_0} \alpha_{n_0 k_0}$ , becomes  $\sum_{n_0 k_0} \alpha_{n_0 k_0}' P_{n_0 k_0} \times (1 - P_k)$ . I place a prime on the  $\alpha$  because the electron bound and continuum wave functions depend on the compression and the temperature. The calculation of these modified  $\alpha$ 's will be described later.

Fourth, a new type of term arises which is added to this sum over  $\alpha$ . Physically this term is due to the appearance of free-free electronic transitions. The free-free transitions describe the excitation of continuum electrons to energies which are higher than the original energies by an amount equal to the energy of the nuclear transition. The excitation rate to the first excited state can be shown to be  $(2J_i+1)(2J_0+1)^{-1} \exp(-E_1/kT)$  times the decay rate of the first excited state.

*Calculation of the temperature and compression-dependent excitation rate.*—In order to calculate the excitation and de-excitation rates, a model for the electron wave functions must be adopted which describes their behavior at high temperatures and compressions. The model chosen here is a modified Thomas-Fermi Model.<sup>2</sup> Briefly, the Dirac equation is solved in a Thomas-Fermi-like potential which goes to zero at the surface of an atomic sphere whose radius is determined by the compression. The continuum is assumed to be depressed to  $E_0$ , the average of the potential seen by an electron over the atomic volume. The number of free electrons,  $N_f$ , is determined from

$$N_f = \frac{2}{3\pi} (kT)^{3/2} \left( \frac{r_0}{a_0} \right)^3 \int_0^\infty \frac{Z^{1/2} dZ}{1 \exp[Z - (\alpha + E_0)/kT]}.$$

This equation assumes a uniform continuum electron density. Here,  $r_0$  is the atomic sphere radius and  $a_0$  is the Bohr radius. The chemical potential,  $\alpha$ , is determined by taking a Fermi-Dirac distribution of all electrons and requiring neutrality of the atom,  $Z = N_f + N_{\text{bound}}$ .

The program CATAR<sup>3</sup> was used with minor corrections to calculate the internal-conversion coefficients for <sup>238</sup>U. The coefficients related to the LI, LII, LIII, MII, MIII, MIV, MV, and NI shells were calculated at the temperatures 0.05, 0.5, 1.0, 1.5, 2.0, 4.0, 7.0, 10.0, 20.0, and 30.0 keV for compressions of 0.3, 1.0, 3.0, 10.0, 30.0, and 100. The corresponding variation of the LIII internal-conversion coefficient is presented in Fig. 1. This coefficient is one of the largest in the sum in Eq. (2). At high tempera-

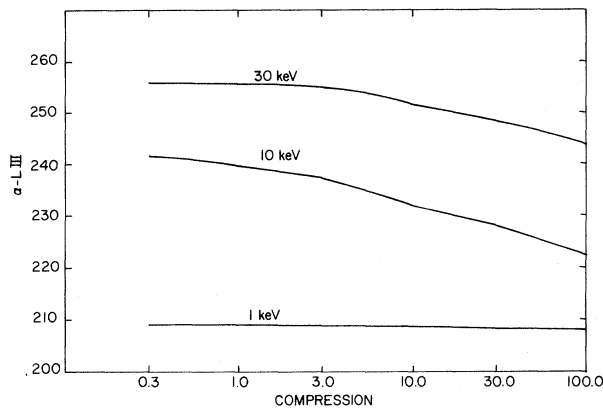


FIG. 1. The L III internal-conversion coefficient for the 45-keV transition of  $^{238}\text{U}$  as a function of temperature and compression.

tures fewer electrons are bound so that the LIII electron is shielded less from the nucleus and is more tightly bound so that its wave function has more overlap with the nucleus. At the higher compressions, more electrons are forced back into bound orbits causing greater shielding and decreasing the coefficient. The internal-conversion coefficients do not scale with the probability of finding the electron at the nucleus as happens at lower ionization levels. This is partly due to

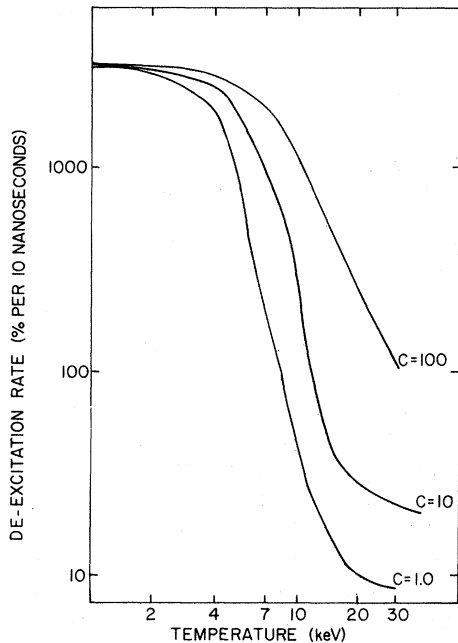


FIG. 2. The  $^{238}\text{U}$  bound-free plus radiative de-excitation rate from the  $2^+$  45-keV excited state to the  $0^+$  ground state.

large changes in binding energy which cause a corresponding change in the available electron phase space.

The de-excitation rate from the first excited 45-keV  $2^+$  state in  $^{238}\text{U}$  as calculated using the appropriately modified form of Eq. (2) is presented in Fig. 2. Only bound-free transitions are included in the sum over internal-conversion coefficients. The rapid decrease of the rate by a few orders of magnitude is caused mostly by the change in the occupation probability of the electron orbits. The half-life at a compression of 1 increases from 0.21 to 76 ns.

The excitation rate from the  $0^+$  ground state to the first excited state is presented in Fig. 3 at compressions of 1, 3, 10, 30, and 100. Here also only the bound-free transitions are included. The compression-1 curve is dominated by radiation excitation which is independent of compression. The other curves have a peak caused by the maximum occurring in the number of electrons available at 45 keV above the electron bound-state energies.

The free-free contribution to the excitation rate, calculated in the Born approximation, is indicated in Fig. 4. It will begin to dominate at higher temperatures. It is expected that the Born approximation is an underestimate of the actual free-free rate.

It has been shown that the low-lying excited states of nuclei can approach their equilibrium populations rapidly under extreme temperature

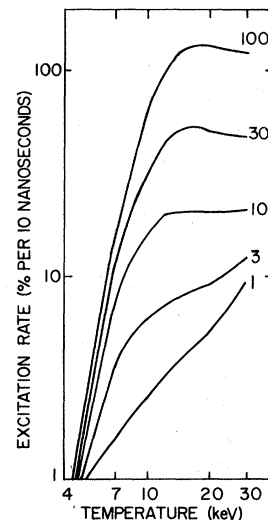


FIG. 3. The  $^{238}\text{U}$  free-bound plus radiative excitation rate from the  $0^+$  ground state to the  $2^+$  45-keV excited state.

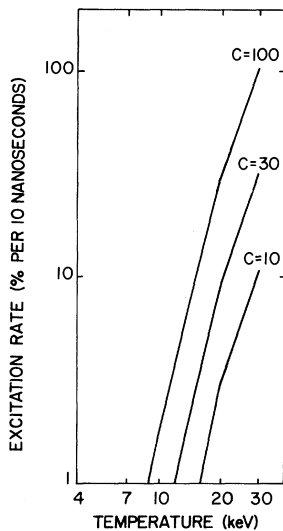


FIG. 4. The  $^{238}\text{U}$  free-free Born approximation excitation rate from the  $0^+$  ground state to the  $2^+$  45-keV excited state.

and compression conditions and that the lifetimes of these excited states can increase by a few orders of magnitude.

The author much appreciates the valuable discussions with Walter Heubner in matters relating to the Thomas-Fermi potential, with Merle Bunker in matters relating to nuclear transition probabilities, and especially with David Liberman in matters relating to electronic transitions. Some results contained herein were obtained using MACSYMA, a symbolic manipulation program developed at Massachusetts Institute of Technology and supported in part by the U. S. Department of Energy under Contract No. E(11-1)-3070 and by the National Aeronautics and Space Administration under Grant No. NSG1323.

<sup>1</sup>H. C. Pauli, K. Alder, and R. M. Steffen, in *The Electromagnetic Interaction in Nuclear Spectroscopy*, edited by W. D. Hamilton (North-Holland, Amsterdam, 1975), pp. 26 and 360. A misprint in the corresponding equation in the book is corrected here.

<sup>2</sup>Richard Latter, *Phys. Rev.* **99**, 1854 (1955).

<sup>3</sup>H. C. Pauli and U. Raff, *Comput. Phys. Commun.* **9**, 392 (1975).

## Protons, Deuterons, and Tritons Emitted from the Reaction of 192-MeV $^{12}\text{C}$ with $^{56}\text{Fe}$

J. B. Ball, C. B. Fulmer, M. L. Mallory,<sup>(a)</sup> and R. L. Robinson

*Oak Ridge National Laboratory, Oak Ridge, Tennessee 37830*

(Received 28 October 1977)

Energy spectra and yields of  $Z=1$  particles from bombardment of an iron target with 192-MeV  $^{12}\text{C}$  ions were measured at a number of angles between  $8^\circ$  and  $65^\circ$ . The spectra extend to energies far above the energy per nucleon of the incident projectile. The observed yields are consistent with an interpretation that projectilelike products of the nuclear collisions are excited sufficiently to evaporate one or more light particles subsequent to the collision.

We report here the results of an experiment to measure the spectra of light particles ( $Z=1$ ) produced by reactions of 16-MeV/nucleon carbon ions with a medium-weight target. These results provide information on the spectral distribution of light particles emitted during intermediate-energy heavy-ion collisions.

The observation of nonstatistical emission of protons from heavy-ion-induced reactions has been noted previously in studies at 8.6 MeV/nucleon<sup>1</sup> and at 10.5 MeV/nucleon.<sup>2</sup> In the work of Galin *et al.*,<sup>1</sup> a forward-peaked "direct" component was subtracted from the proton spectra be-

fore treating the observed angular distributions in terms of a statistical decay of the compound system. Britt and Quinton<sup>2</sup> reported a similar forward-peaked component in the proton spectra and concluded that the major process involved in producing this direct component was the breakup of the incident projectile during a grazing collision with the target nucleus. Such a fragmentation process does not explain the light-particle spectra observed in the present study of the  $^{12}\text{C}$  on  $^{56}\text{Fe}$  reaction at 16 MeV/nucleon. For example, the protons were found to have energies up to 4 times the average laboratory energy of the